arXiv:1403.6603v1 [astro-ph.SR] 26 Mar 2014

Emission line variability in the spectrum of V417 Centauri ⋆

K. A. Stoyanov[1]⋆⋆, R. K. Zamanov[1], M. F. Bode[2], J. Pritchard[3], N. A. Tomov[1], A. Gomboc[4,5], K. Koleva[1]

[1] Institute of Astronomy and National Astronomical Observatory, Bulgarian Academy of Sciences, 72 Tsarighradsko Shousse Blvd., 1784 Sofia, Bulgaria

[2] Astrophysics Research Institute, Liverpool John Moores University, IC2 Liverpool Science Park, 146 Brownlow Hill, Liverpool L3 5RF, UK

[3] European Southern Observatory, Karl-Schwarzschild-Str. 2, D-85748 Garching bei München, Germany

[4] Faculty of Mathematics and Physics, University of Ljubljana, Jadranska 19, 1000 Ljubljana, Slovenia

[5] Centre of Excellence SPACE-SI, Aškerčeva cesta 12, SI-1000, Ljubljana, Slovenia

(Research report. Accepted on xx.xx.xxxx)

Abstract. We report high resolution ($\lambda/\Delta\lambda \sim 48000$) spectral observations of the yellow symbiotic star V417 Cen obtained in 2004. We find that the equivalent widths of the emission lines decreased, while the brightness increased. The FWHMs and wavelengths of the emission lines do not change.

We estimated the interstellar extinction towards V417 Cen as $E_{B-V} = 0.95 \pm 0.10$, using the KI interstellar line.

Using the [O III] lines, we obtain a rough estimation of the density and the temperature in the forbidden lines region $\log N_e \approx 4.5 \pm 0.5$ and $T_e = 100000 \pm 25000$ K. Tidal interaction in this binary is also discussed.

Key words: stars: individual: V417 Cen – binaries: symbiotic

1 Introduction

Symbiotic stars (SSs) are thought to comprise a compact object (usually a white dwarf) accreting from a cool giant. They offer a laboratory in which to study such processes as (1) mass loss from cool giants and the formation of nebulae, (2) accretion onto compact objects, radiative transfer in gaseous nebulae, (3) jets and outflows (i.e. Corradi, Mikolajewska & Mahoney 2003).

V417 Centauri (HV 6516, Hen 3-977) is a poorly studied D'-type (yellow) symbiotic system surrounded by a faint asymmetric nebula. The symbiotic nature of the object was proposed by Steiner, Cieslinski & Jablonski (1988). The cool component is a G2 Ib-II star, with $\log(L/L_\odot) = 3.5$ and $T_{eff} = 5000$ K (van Winckel et al. 1994). Pereira, Cunha & Smith (2003) found atmospheric parameters $T_{eff} = 6000$, $\log g = 3.0$, and spectral type F9 III/IV.

The binary period is not defined. Van Winckel et al. (1994) found a 245.68 day periodicity with an amplitude of 0.5 mag using Harvard and Sonneberg plates. Gromadzki et al. (2011) using optical photometric observations covering 20 years detected strong long term modulation with a period of about 1700 days and amplitude about 1.5 mag in V-band, in addition to variations with shorter time-scales and lower amplitudes. However, the long period seems to be non-coherent and the nature of light variations and the length of the orbital period remain unknown.

⋆ based on data from ESO (program 073.D-0724) and AAVSO

⋆⋆ e-mail: kstoyanov@astro.bas.bg

Here we discuss the emission line variability of V417 Cen in 2004.

2 Observations

We secured 8 spectra in 2004 using the ESO, La Silla, 2.2m telescope and the FEROS spectrograph. FEROS is a fibre-fed echelle spectrograph, providing a resolution of $\lambda/\Delta\lambda$=48000, wide wavelength coverage from about 4000 Å to 8000 Å in one exposure and a high detector efficiency (Kaufer et al. 1999). The log of observations is given in Table 1, and the measured emission line parameters in Table 2. The typical errors in the equivalent widths are ±10% for the strong lines (EW>3 Å) and ±20% for the weaker lines (EW $\lesssim$ 3 Å). Errors for the fluxes are typically 10% and 20%; FWHM around 0.02 - 0.10 Å, and for wavelengths about 0.1 Å. On Fig. 3 are plotted spectra, obtained during three nights. The spectrum from June 3, 2004 is almost identical to the spectrum in July 1993 (see Fig.3 of Van Winckel et al. 1994).

3 Interstellar extinction towards V417 Cen

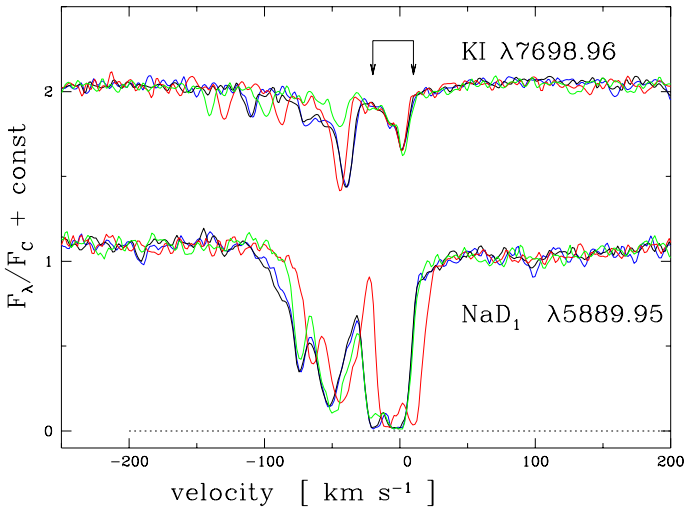

Fig. 1. The lines KI λ7699.96 (upper) and NaD λ5889.95 (lower plot). The spectra are normalized to the local continuum. The blue line represents sp1, the black line - sp3, the red line - sp5, and the green line - sp8. The arrows indicate the non-variable part of the KI line, on which basis we estimate $E_{B-V} = 0.95 \pm 0.10$ (see the text).

The NaD_1 and NaD_2 lines as well as the KI λ7699 line are visible in our spectra and are plotted in Fig.1. A clear variability is visible indicating that they have both stellar and interstellar origin. NaD lines are saturated and inappropriate for calculation of the interstellar extinction. We do detect a non-variable part in KI λ7699 which has EW (KI λ7698.965) ≈ 0.24 Å. Following the calibration of Munari & Zwitter (1997) this corresponds to $E_{B-V} = 0.95$ ± 0.10. This value is similar to the previous estimates of $E_{B-V} = 1.15$ (Van Winckel et al. 1994, obtained on the basis of HI line ratios) and $E_{B-V} \sim 0.7$ (Cieslinski, Elizalde & Steiner 1994 from the photometric colours).

Table 1. Log of observations of V417 Cen. In the table are given the number of the spectrum, date of observations, Julian Day, and exposure time.

N:	Date	JD	exptime
	yyyy-mm-dd	2400000+	[sec]
sp1	2004-04-12	53107.254	600
sp2	2004-04-12	53107.262	600
sp3	2004-04-14	53109.273	600
sp4	2004-04-14	53109.280	600
sp5	2004-06-03	53159.188	600
sp6	2004-06-03	53159.195	600
sp7	2004-07-21	53207.006	600
sp8	2004-07-21	53207.013	600

4 Tidal interaction between the components

The physics of tidal interaction for stars with convective envelopes has been analyzed by several authors. We use the estimate from Zahn (1977, 1989). The synchronization timescale in terms of the period is

$$\tau_{\rm syn} \approx 800 \left(\frac{M_{\rm g} R_{\rm g}}{L_{\rm g}} \right)^{1/3} \frac{M_{\rm g}^2 (\frac{M_{\rm g}}{M_{\rm wd}} + 1)^2}{R_{\rm g}^6} P_{\rm orb}^4 \ \ {\rm yr}, \qquad (1)$$

where $M_{\rm g}$ and $M_{\rm wd}$ are the masses of the giant and white dwarf respectively in Solar units, and $R_{\rm g}$, $L_{\rm g}$ are the radius and luminosity of the giant, also in Solar units. The orbital period $P_{\rm orb}$ is measured in days.

Following Hurley, Tout & Pols (2002), the circularization time scale is:

$$\frac{1}{\tau_{\rm circ}} = \frac{21}{2} \left(\frac{k}{T} \right) q_2 (1 + q_2) \left(\frac{R_{\rm g}}{a} \right)^8 . \qquad (2)$$

where the mass ratio $q_2 = M_{\rm wd}/M_{\rm g}$. In Eq. 2, (k/T) is derived from Rasio et al. (1996), where k is an apsidal motion constant and T is the timescale on

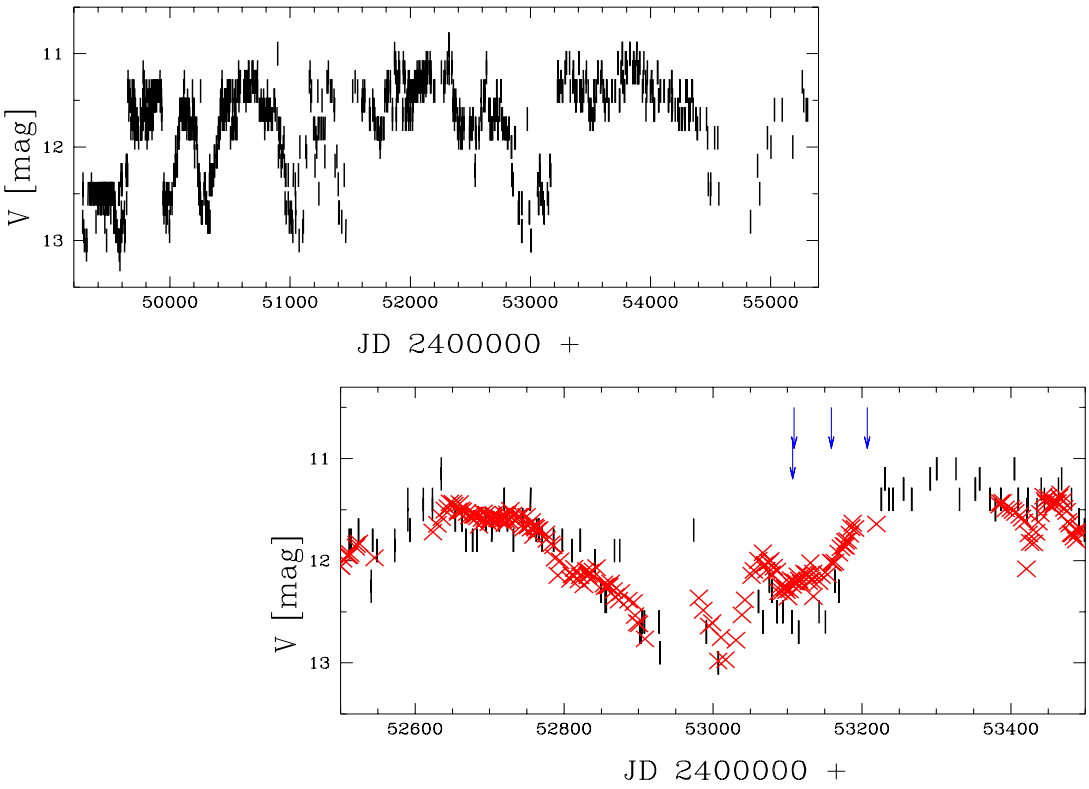

Fig. 2. Brightness variability of V417 Cen from American Association of Variable Star Observers (AAVSO) and ASAS observations. The (black) lines indicates the data from AAVSO and the (red) crosses - the data from ASAS. The arrows indicate the time of our spectroscopic observations.

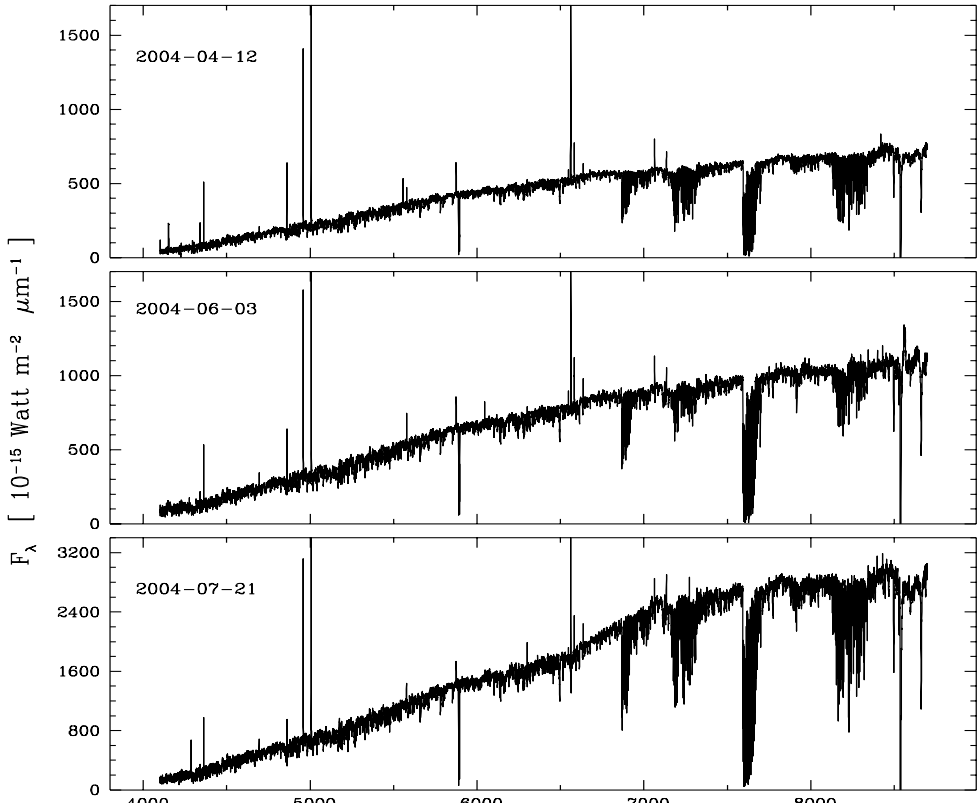

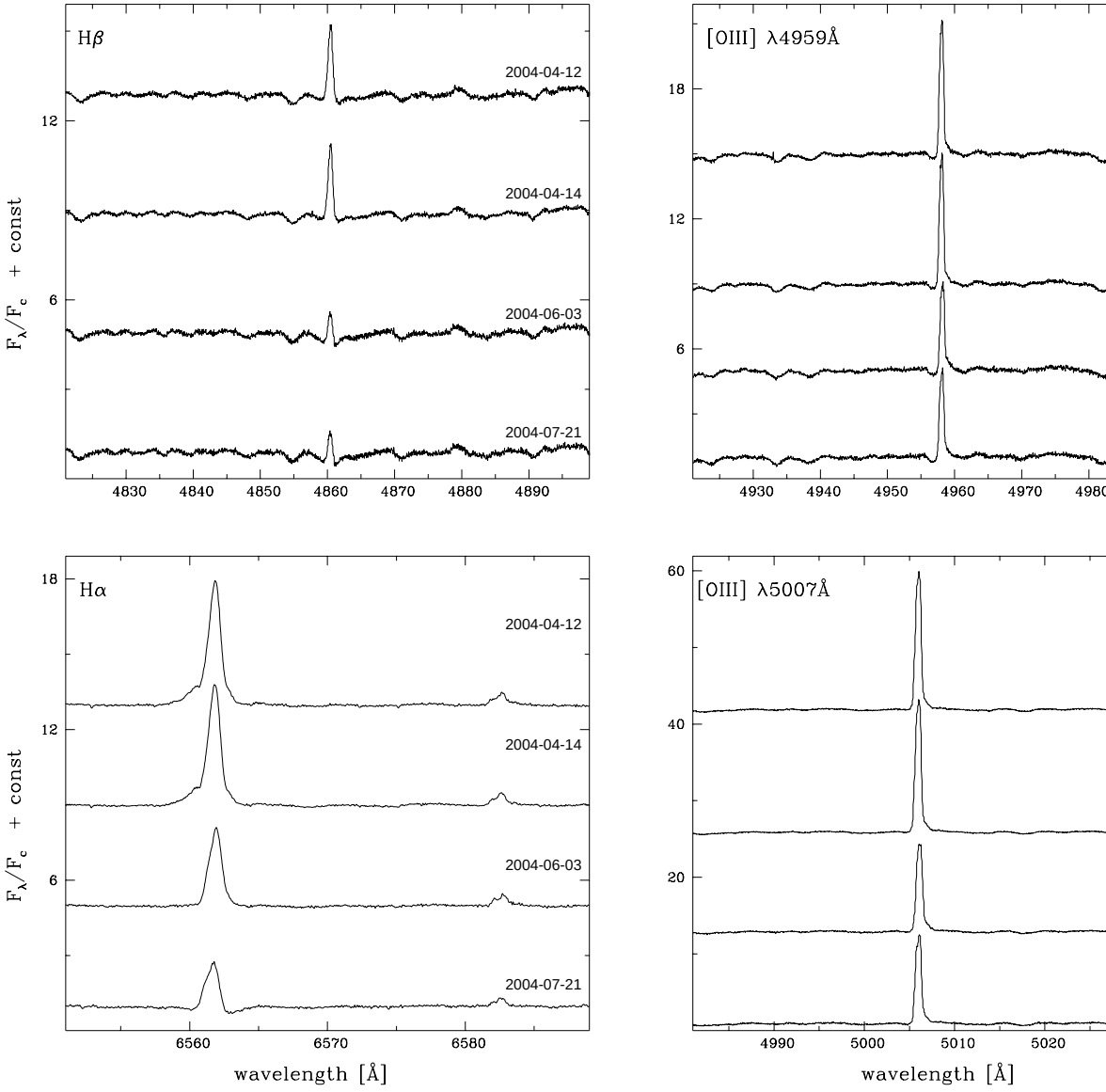

Fig. 4. The Hβ, Hα (left), [OIII]λ4959 and [OIII]λ5007 (right) emission lines of V417 Cen. All spectra are are normalized to the local continuum.

Table 2. Optical emission line parameters. The typical errors in the equivalent widths and fluxes are ±10% for the strong lines (EW>3 Å) and ±20% for the weaker lines (EW $\lesssim$ 3 Å).

spec No:		sp1	sp2	sp3	sp4	sp5	sp6	sp7	sp8
		JD53107		JD53109		JD53159		JD53207	
Equivalent Widths [Å]									
4101	Hδ	1.04	0.87	1.24	1.14	0.33	0.32	0.07	0.14
4340	Hγ	2.57	2.20	2.78	2.19	1.24	1.26	0.96	0.99
4363	[O III]	2.95	2.44	2.45	2.33	1.52	1.41	1.47	1.55
4861	Hβ	2.88	3.07	2.67	2.75	1.64	1.60	1.56	1.39
4959	[O III]	4.59	4.76	4.37	4.78	3.33	3.43	3.23	3.01
5007	[O III]	13.89	13.68	13.97	13.08	9.85	9.72	9.53	9.05
5876	He I	0.48	0.49	0.52	0.51	0.32	0.25	0.18	0.20
6548	[N II]	0.11	0.11	0.12	0.12	0.16	0.10	0.07	0.06
6563	Hα	6.53	6.37	6.10	6.16	3.55	3.48	3.04	2.84
6584	[N II]	0.54	0.46	0.48	0.44	0.43	0.34	0.27	0.30
7065	He I	0.47	0.54	0.57	0.55	0.34	0.21	0.19	0.16
7135	[Ar III]	0.27	0.25	0.30	0.31	0.24	0.24	0.18	0.18
FWHM [Å]									
4101	Hδ	0.78±0.05	0.84±0.05	0.90±0.05	0.65±0.06	0.8±0.4:	0.6±0.3:	—	1.0±0.4:
4340	Hγ	0.67±0.01	0.74±0.03	0.75±0.02	0.75±0.02	0.73±0.02	0.81±0.02	0.65±0.01	0.73±0.05
4363	[O III]	0.51±0.01	0.50±0.01	0.51±0.01	0.52±0.01	0.56±0.02	0.51±0.02	0.53±0.01	0.52±0.03
4861	Hβ	0.80±0.01	0.82±0.01	0.80±0.01	0.81±0.01	0.77±0.02	0.78±0.02	0.53±0.01	0.78±0.01
4959	[O III]	0.69±0.01	0.69±0.01	0.70±0.01	0.70±0.01	0.73±0.02	0.76±0.01	0.74±0.01	0.74±0.02
5007	[O III]	0.70±0.01	0.69±0.01	0.70±0.01	0.72±0.01	0.75±0.01	0.75±0.01	0.75±0.01	0.74±0.01
5876	He I	0.96±0.02	0.94±0.02	1.05±0.07	1.01±0.03	1.07±0.04	0.96±0.02	0.91±0.04	1.27±0.04
6548	[N II]	0.70±0.08	0.86±0.05	0.88±0.10	1.12±0.10	1.30±0.15	0.95±0.10	1.0±0.2:	1.3 ±0.3:
6563	Hα	1.15±0.01	1.10±0.02	1.11±0.01	1.09±0.01	1.11±0.01	1.11±0.02	1.16±0.05	1.16±0.01
6584	[N II]	1.10±0.10	1.14±0.04	1.11±0.02	1.09±0.10	1.17±0.05	1.12±0.05	0.94±0.03	1.08±0.04
7065	He I	1.43±0.05	1.45±0.07	1.49±0.03	1.56±0.04	1.10±0.10	1.24±0.02	1.25±0.03	1.39±0.10
7135	[Ar III]	1.28±0.08	1.27±0.08	1.14±0.02	1.16±0.02	1.06±0.10	1.17±0.04	1.28±0.06	1.38±0.04
Optical emission line fluxes [erg cm^{-2} s^{-1}]									
4101	Hδ	9.39E-15	6.39E-15	7.73E-15	7.07E-15	1.73E-15	3.06E-15	6.52E-16	2.70E-15
4340	Hγ	1.82E-14	1.76E-14	2.06E-14	1.92E-14	1.14E-14	1.39E-14	1.13E-14	1.28E-14
4363	[O III]	3.40E-14	3.31E-14	3.21E-14	3.14E-14	2.66E-14	2.46E-14	3.84E-14	3.92E-14
4861	Hβ	6.00E-14	6.12E-14	6.00E-14	5.74E-14	4.06E-14	4.44E-14	3.89E-14	3.68E-14
4959	[O III]	1.30E-13	1.37E-13	1.36E-13	1.34E-13	1.11E-13	1.23E-13	1.55E-13	1.53E-13
5007	[O III]	4.20E-13	4.33E-13	4.23E-13	4.09E-13	3.59E-13	3.63E-13	4.77E-13	4.64E-13
5876	He I	2.86E-14	2.67E-14	3.21E-14	3.20E-14	2.16E-14	2.41E-14	1.80E-14	2.00E-14
6548	[N II]	7.39E-15	7.44E-15	8.35E-15	9.41E-15	1.06E-14	6.64E-15	8.82E-15	7.29E-15
6563	Hα	5.61E-13	5.66E-13	5.24E-13	5.32E-13	3.02E-13	3.21E-13	3.02E-13	2.91E-13
6584	[N II]	4.51E-14	3.96E-14	4.61E-14	4.71E-14	3.73E-14	2.90E-14	3.46E-14	3.99E-14
7065	He I	4.69E-14	4.81E-14	4.76E-14	4.90E-14	2.46E-14	2.91E-14	2.82E-14	2.21E-14
7135	[Ar III]	2.22E-14	2.10E-14	2.88E-14	3.02E-14	2.10E-14	1.69E-14	2.74E-14	2.69E-14
Emission line peak observed wavelengths [Å]									
4101	Hδ	4100.98	4100.97	4101.03	4100.97	4101.09	4101.05	4101.08	4100.94
4340	Hγ	4339.66	4339.65	4339.64	4339.66	4339.78	4339.75	4339.67	4339.62
4363	[O III]	4362.38	4362.38	4362.37	4362.37	4362.46	4362.45	4362.36	4362.36
4861	Hβ	4860.44	4860.44	4860.43	4860.43	4860.54	4860.54	4860.40	4860.39
4959	[O III]	4958.07	4958.07	4958.07	4958.06	4958.21	4958.21	4958.10	4958.10
5007	[O III]	5005.98	5005.99	5005.98	5005.97	5006.12	5006.12	5006.01	5006.00
5876	He I	5874.65	5874.63	5874.63	5874.63	5874.77	5874.76	5874.58	5874.65
6548	[N II]	6547.30	6547.33	6547.28	6547.29	6547.40	6547.42	6547.36	6547.30
6563	Hα	6561.72	6561.73	6561.71	6561.71	6561.87	6561.87	6561.61	6561.61
6584	[N II]	6582.58	6582.57	6582.56	6582.56	6582.67	6582.68	6582.52	6582.58
7065	He I	7063.86	7063.85	7063.81	7063.82	7064.01	7064.01	7063.91	7063.83
7135	[Ar III]	7134.67	7134.67	7134.61	7134.61	7134.90	7134.84	7134.72	7134.64

which significant changes in the orbit take place through tidal evolution:

$$\left(\frac{k}{T}\right) = \frac{2}{21}\frac{f_{\rm conv}}{\tau_{\rm conv}}\frac{M_{\rm env}}{M_{\rm g}}\ {\rm yr}^{-1}, \tag{3}$$

where $M_{\rm env}$ is the envelope's mass, and

$$\tau_{\rm conv} = 0.4311\left(\frac{M_{\rm env}R_{\rm env}(R_{\rm g}-\frac{1}{2}R_{\rm env})}{3L_{\rm g}}\right)^{\frac{1}{3}}{\rm yr} \tag{4}$$

where $R_{\rm env}$ is the depth of the convective envelope. $\tau_{\rm conv}$ is the eddy turnover time scale (the time scale on which the largest convective cells turnover). The numerical factor $f_{\rm conv}$ is

$$f_{\rm conv} = \min\left[1, \left(\frac{P_{\rm tid}}{2\tau_{\rm conv}}\right)^2\right], \tag{5}$$

where $P_{\rm tid}$ is the tidal pumping time scale given by

$$\frac{1}{P_{\rm tid}} = \left|\frac{1}{P_{\rm orb}} - \frac{1}{P_{\rm rot}}\right|. \tag{6}$$

From Hut (1981) we can estimate the $\tau_{\rm al}$ to $\tau_{\rm circ}$ ratio:

$$\frac{\tau_{\rm al}}{\tau_{\rm circ}} = \frac{7}{\alpha+3}. \tag{7}$$

where $\tau_{\rm al}$ is alignment time scale and α is a dimensionless quantity, representing the ratio of the orbital and rotational angular momentum:

$$\alpha = \frac{q_2}{1+q_2}\frac{1}{r_{\rm g}^2}\left(\frac{a}{R_{\rm g}}\right)^2, \tag{8}$$

where $r_{\rm g}$ is the gyration radius of the giant. For stars with similar stellar parameters, the gyration radius is $r_{\rm g}$=0.14 (Claret 2007).

We assume for the red giant $R_{\rm env} = 0.9\ R_{\rm g}$ and $M_{\rm env} = 3.0\ M_{\odot}$ (Herwig 2005). Using stellar parameters R_g=$75R_{\odot}$, M_g=$6M_{\odot}$, L_g=$3160L_{\odot}$and M_{wd}=$0.75M_{\odot}$(Gromadzki et al. 2011), we calculate $P_{\rm tid} = 50$ days, $f_{\rm conv} = 1$, $\tau_{\rm conv} = 0.29$ yr, and $(k/T) = 0.055\ {\rm yr}^{-1}$. From Eq. 1, Eq. 2 and Eq. 7 we calculate the tidal time scales.

If $P_{orb} = 1700$ d, then the synchronization time scale $\tau_{\rm sync} = 5.75\times10^7$ yr; the circularization timescale $\tau_{\rm circ} = 1.4\times10^{10}$ yr; the alignment timescale $\tau_{\rm al} = 6.5\times10^7$ yr; the pseudo-synchronization time scale $\tau_{\rm ps} = 2.2\times10^7$ yr, and the tidal force does not play an important role.

If $P_{orb} = 245.68$ d, then $\tau_{\rm sync} = 2.5 \times 10^4$ yr, $\tau_{\rm circ} = 4.6 \times 10^5$ yr, $\tau_{\rm al} = 2.8 \times 10^4$ yr, $\tau_{\rm ps} = 1 \times 10^4$ yr, and the orbital eccentricity could be as high as $e \approx 0.64$, if the system is pseudo-synchronized.

Corradi & Schwarz (1997) obtained 4000 yr for the age of the nebula around AS 201, and 40000 yr for that around V417 Cen. This means that the tidal force plays important role only if the shorter photometric period ($\sim$ 250 d) is the orbital one.

5 Emission lines and spectral line variability in 2004

5.1 Diagnostic diagram $\lambda5007/H\beta$ vs. $\lambda4363/H\gamma$

The diagnostic diagram $\lambda5007/H\beta$ vs. $\lambda4363/H\gamma$ for 174 flux measurements (planetary nebulae, S,D,D'-type symbiotic stars, and 6 peculiar objects) is presented by Baella (2010).

We calculate the ratio $R_1 = \lambda5007/H\beta = 4.95, 4.47, 5.37, 5.19$ and $R_2 = \lambda4363/H\gamma = 1.016, 0.916, 0.832, 1.154$ for JD 2453107, JD 2453109, JD 2453159, JD 2453207 respectively. For every JD we use the average value from the two spectra obtained in the night. This corresponds to $4.5 < R_1/R_2 < 6.4$. However the symbiotic limit is $R_1/R_2 \leq 3$ (see Fig.1 of Baella 2010). This means that V417 Cen is located above the symbiotic limit - somewhere between symbiotics and peculiar objects.

5.2 Density and temperature of the forbidden lines region

In the Table 2 are listed the emission lines we observe in the spectrum. The critical densities of the forbidden lines, N_{cr}, are as follows: $\log N_{cr} = 7.5$ for [O III]λ4363, $\log N_{cr} = 5.8$ for [O III]λ5007, $\log N_{cr} = 4.9$ for [N II]λ6584, $\log N_{cr} = 6.7$ for [Ar III]λ7135 (Appenzeller & Oestreicher, 1988). We do not detect emission lines with $\log N_{cr} < 4.9$ (e.g. [S II]λ6730), and we estimate the density of the forbidden lines region $\log N_e \approx 4.5 \pm 0.5$.

Using the latest collision strengths and line ratios for forbidden [O III] lines (Palay et al. 2012, Nahar & Ethan, private communication), we obtain an estimation of the temperature in the forbidden lines region in the range $T_e = 75000 - 130000$ K (for $\log N_e \approx 4.5$). It seems that there is a tendency for T_e to decrease as the brightness increases.

5.3 Emission lines variability

The emission line spectrum of V417 Cen is strongly variable. In 1988 only [O III] and He I lines were seen in emission; in 1993 the Balmer lines and [N II] were also pronounced (Van Winckel et al. 1994). In the low resolution spectra taken in 1996 the intensity of [O III] lines dramatically decreased and seemed similar to Hα (Munari & Zwitter 2002).

The photometric variability of the object at the time of our spectroscopic observations is shown in Fig.2. The photometric data are taken from AAVSO. During the time of our observations, the brightness of the star varied as follows: at MJD2453107-2453109 V$\approx$12.6-12.7, at MJD2453159 V$\approx$12.3 and at

MJD2453207 V≈11.4 mag. We had the chance to obtain spectra during the time of brightness changes. The brightness variability has been accompanied by changes in the emission lines. The variability of the Hα line is immediately apparent (see Fig.4 and Table.1). When the brightness of the star was 12.6-12.7 mag, the Hα emission line had equivalent width EW$_{H\alpha} \approx 6.4 \pm 0.2$ Å and FWZI $\approx$ 290 km s^{-1}, with the line extending at zero intensity from -228 to +56 km s^{-1}and FWHM $\approx$ 52 km s^{-1}. When the star was brighter, at $\approx$ 11.3 mag, then EW$_{H\alpha} \approx 2.9$ Å and FWZI $\approx$ 130 km s^{-1}, extending from -126 to +2 km s^{-1}, but with FWHM remaining practically the same.

The Balmer emission lines, appearing in the extended envelopes of symbiotic stars usually have an ordinary nebular profile with typical FWHM $\approx$ 100-150 km s^{-1}, for example AG Dra (Tomova & Tomov 1999). FWHM increases to 200 km s^{-1} only during the active phase. The basic mechanism determining their width is turbulence in the gas. The central narrow emission of V417 Cen is very similar. The appearance and the variability of the narrow component is relatively common in symbiotic stars (see also Ikeda & Tamura 2004 and references therein).

It seems that the optical fluxes of the Balmer lines decrease, while the brightness increased. The fluxes of the forbidden lines ([O III] λ4363, λ4959, λ5007, [N II] λ6548, λ6584, [Ar III] λ7135) seem to remain almost constant. The EWs of both Balmer and forbidden lines decreased, while the brightness increased. The measured wavelengths of the emission lines are constant within the observational errors. All fluxes and equivalent widths are measured by measuring the whole emission line profiles.

6 Discussion

The Balmer emission lines, appearing in the extended envelopes of symbiotic stars, usually have an ordinary nebular profile with typical FWHM $\approx$ 100-150 km s^{-1}, for example AG Dra (Tomova & Tomov 1999). FWHM increases to 200 km s^{-1} only during the active phase. The basic mechanism determining their width is turbulence in the gas. The appearance and the variability of the narrow component is relatively common in symbiotic stars (see also Ikeda & Tamura 2004 and the references therein). The central narrow emission of V417 Cen is very similar.

When the star brightness increases, the EW of the line decreases. The FWHM and line fluxes of the Balmer lines remain unchanged. Our interpretation is that the continuum of G2 Ib-II supergiant was obscured by dust and after it the dust absorption decreased. In other words, during the time of the light minimum the G9 supergiant spectrum is veiled by dust.

Rapid rotation is a common property of the cool components of D' SSs (Jorissen et al. 2005, Zamanov et al. 2006). This fast rotation is due to the mass transfer (spin accretion from the former AGB) and/or the tidal force (Soker 2002; Ablimit & Lü 2012). Fast rotation in D'-type symbiotics probably leads to the formation of a circumstellar disk as in the classical Be stars, where the fast rotation of the B star expels matter in the equatorial regions (see Porter & Rivinius 2003). The geometry and kinematics of the circumstellar environment in Be stars is best explained by a rotationally supported relatively thin disk

with very little outflow. The central B star is a fast rotator with a commonly quoted mean value of about 70% - 80% of the critical velocity, i.e. the ratio $v_{rot}/v_{cr} \sim 0.7$. Regarding the ratio $v_{rot}/v_{cr} \sim 0.7$ the rotation of the G2Ib-II component is similar to the Be stars. This is estimated as $v\,sin\,i = 75$ km s^{-1}, which is 71% of the critical value and implies a short rotation period of the mass donor $P_{rot} \leq 51$ d (Zamanov et al. 2006). By analogy with the Be stars and Be/X-ray binaries, we expect a rotationally supported disk around the supergiant in V417 Cen with little outflow.

The far-IR data (Kenyon, Fernandez-Castro & Stencel 1988) for D'-type symbiotics indicate optically thick dust clouds, with temperature $T_{dust} \sim 100-400$ K (Kenyon, Fernandez-Castro & Stencel 1988). The IR colours of V417 Cen reveal the presence of warmer dust more similar to D-type symbiotics. The IR energy distribution peaks in the L band (3.79 μm), corresponding to a dust temperature of 800 K. The infrared excess is broad and cannot be fitted with a single black body, indicating temperature stratification in the dust (van Winckel et al. 1994). Angeloni et al. (2007), for another D'-type symbiotic HD330036, detected three dust shells, which are probably circumbinary.

The IR energy distribution of V417 Cen is similar to the distribution in D-type symbiotics with resolved bipolar nebulae like BI Cru, He 2-104 and R Aqr (Schwarz & Corradi 1992), with a broad IR excess peaking in the L band. In these systems, an excretion disk is thought to provide equatorial density enhancement.

Where is the dust located? There are three suggestions for this:

- The hot component lies outside the dust shell that enshrouds the giant companion (as suggested for D-type symbiotics by Kenyon, Fernandez-Castro & Stencel 1986).
- The dust is located around the hot component and at L_4 and L_5 Lagrangian points (Gromadzki et al. 2011).
- Dust shells are circumbinary, i.e. the orbital period is short and the supergiant and WD are in the centre of the dust shells, as supposed by Angeloni et al. (2007) for HD330036.

Conclusion

We report 8 high resolution spectra of the D'-type symbiotic star V417 Cen obtained between April - July 2004, when the star's V-band brightness increased from 12.4^m to 11.5^m.

We find that the equivalent widths of the emission lines decreased, while the brightness increased. The FWHMs and wavelengths of the emission lines do not change.

It seems that the fluxes of the observed Balmer lines ($H\alpha$, $H\beta$, $H\gamma$) decreased by 20%, while the brightness increased. The fluxes of the forbidden lines ([O III]λ4363, λ4959, λ5007, [N II] λ6548, λ6584, [Ar III] λ7135) remained almost constant.

On the basis of the KI λ7698.965 interstellar line, the interstellar extinction towards V417 Cen is estimated as $E_{B-V} = 0.95 \pm 0.10$.

Using the [O III] lines, we obtain a rough estimation of the density and the temperature in the forbidden line region $\log N_e \approx 4.5 \pm 0.5$ and $T_e = 100000 \pm 25000$ K.

Acknowledgments

We thank the anonymous referee for constructive comments. This work was supported in part by the OP "HRD", ESF and Bulgarian Ministry of Education and Science under the contract BG051PO001-3.3.06-0047. AG acknowledges funding from the Slovenian Research Agency and from the Centre of Excellence for Space Sciences and Technologies SPACE-SI, an operation partly financed by the European Union, European Regional Development Fund and Republic of Slovenia, Ministry of Education, Science and Sport.

References

[2012]Ablimit, I., Lü, G L., 2012, Sci. Chi.: Phys.Mech. Astron. 56, 663
[2007]Angeloni, R., Contini, M., Ciroi, S., & Rafanelli, P. 2007, A&A, 472, 497
[Appenzeller & Oestreicher(1988)]Appenzeller, I., & Oestreicher, R. 1988, AJ, 95, 45
[Baella(2010)]Baella, N. O. 2010, IAU Symposium, 262, 307
[Cieslinski et al.(1994)]Cieslinski, D., Elizalde, F., & Steiner, J. E. 1994, A&AS, 106, 243
[Claret(2007)]Claret, A. 2007, A&A 467, 1389
[Corradi et al.(2003)]Corradi, R. L. M., Mikolajewska, J., & Mahoney, T. J. 2003, Symbiotic Stars Probing Stellar Evolution, Astronomical Society of the Pacific Conference Series, 303
[Corradi & Schwarz(1997)]Corradi, R., & Schwarz, H. E. 1997, Physical Processes in Symbiotic Binaries and Related Systems, 147
[Frankowski & Jorissen(2007)]Frankowski, A., & Jorissen, A. 2007, BaltA, 16, 104
[Gromadzki et al.(2011)]Gromadzki, M., Mikolajewska, J., Pilecki, B., Whitelock, P., & Feast, M. 2011, Asymmetric Planetary Nebulae 5 Conference, A. A. Zijlstra, F. Lykou, I. McDonald, and E. Lagadec, eds., 63P
[Herwig(2005)]Herwig, F. 2005, ARA&A, 43, 435
[Hurley et al.(2002)]Hurley, J. R., Tout, C. A., & Pols, O. R. 2002, MNRAS, 329, 897
[Hut(1981)]Hut, P. 1981, A&A, 99, 126
[Ikeda & Tamura(2004)]Ikeda, Y., & Tamura, S., 2004, PASJ, 56, 353
[Jorissen et al.(2005)]Jorissen, A., Začs, L., Udry, S., Lindgren, H., & Musaev, F. A. 2005, A&A, 441, 1135
[Kaufer et al.(1999)]Kaufer, A., Stahl, O., Tubbesing, S., Norregaard, P., Avila, G., Francois, P., Pasquini, L., & Pizzella, A. 1999, The Messenger, 95, 8
[Kenyon et al.(1986)]Kenyon, S. J., Fernandez-Castro, T., & Stencel, R. E. 1986, AJ, 92, 1118
[Kenyon et al.(1988)]Kenyon, S. J., Fernandez-Castro, T., & Stencel, R. E. 1988, AJ, 95, 1817
[Munari & Zwitter(1997)]Munari, U., & Zwitter, T. 1997, A&A, 318, 269
[Munari & Zwitter(2002)]Munari, U., & Zwitter, T. 2002, A&A, 383, 188
[Palay et al.(2012)]Palay, E., Nahar, S. N., Pradhan, A. K., & Eissner, W. 2012, MNRAS, 423, L35
[Pereira et al.(2003)]Pereira, C. B., Cunha, K., & Smith, V. V. 2003, Symbiotic Stars Probing Stellar Evolution, 303, 85
[Porter & Rivinius(2003)]Porter, J. M., & Rivinius, T. 2003, PASP, 115, 1153
[Rasio et al.(1996)]Rasio, F. A., Tout, C. A., Lubow, S. H., & Livio, M. 1996, ApJ, 470, 1187
[Soker(2002)]Soker, N. 2002, MNRAS, 337, 1038
[Steiner et al.(1988)]Steiner, J. E., Cieslinski, D., & Jablonski, F. J., 1988, Progress and Opportunities in Southern Hemisphere Optical Astronomy. The CTIO 25th Anniversary Symposium, 1, 67
[Schwarz & Corradi(1992)]Schwarz, H. E., & Corradi, R. L. M. 1992, A&A, 265, L37
[Tomova & Tomov(1999)]Tomova, M. T., & Tomov, N. A., 1999, A&A, 347, 151
[Van Winckel et al.(1994)]Van Winckel, H., Schwarz, H. E., Duerbeck, H. W., & Fuhrmann, B., 1994, A&A, 285, 241
[Zahn(1977)]Zahn, J.-P. 1977, A&A, 57, 383
[Zahn(1989)]Zahn, J.-P. 1989, A&A, 220, 112
[Zamanov et al.(2006)]Zamanov, R. K., Bode, M. F., Melo, C. H. F., et al. 2006, MNRAS, 365, 1215